Journal of Medicinal Chemistry

ARTICLE

pubs.acs.org/jmc

Structure-Based Design of Pseudopeptidic Inhibitors for SIRT1 and SIRT2

Tero Huhtiniemi,[†,‡] Heikki S. Salo,[*,†,‡] Tiina Suuronen,[§] Antti Poso,[†] Antero Salminen,[§,∥] Jukka Leppänen,[†] Elina Jarho,[†,⊥] and Maija Lahtela-Kakkonen[†]

[†]School of Pharmacy and [§]Department of Neurology, Institute of Clinical Medicine, University of Eastern Finland, P.O. Box 1627, 70211 Kuopio, Finland

[∥]Department of Neurology, Kuopio University Hospital, P.O. Box 1777, 70211 Kuopio, Finland

[⊥]Department of Chemistry, Medicinal Chemistry, University of Gothenburg, 41296 Gothenburg, Sweden

Supporting Information

ABSTRACT: The lack of substrate-bound crystal structures of SIRT1 and SIRT2 complicates the drug design for these targets. In this work, we aim to study whether SIRT3 could serve as a target structure in the design of substrate based pseudopeptidic inhibitors of SIRT1 and SIRT2. We created a binding hypothesis for pseudopeptidic inhibitors, synthesized a series of inhibitors, and studied how well the fulfillment of the binding criteria proposed by the hypothesis correlated with the in vitro inhibitory activities. The chosen approach was further validated by studying docking results between 12 different SIRT3, Sir2Tm, SIRT1 and SIRT2 X-ray structures and homology models in different conformational forms. It was concluded that the created binding hypothesis can be used in the design of the substrate based inhibitors of SIRT1 and SIRT2 although there are some reservations, and it is better to use the substrate-bound structure of SIRT3 instead of the available apo-SIRT2 as the target structure.

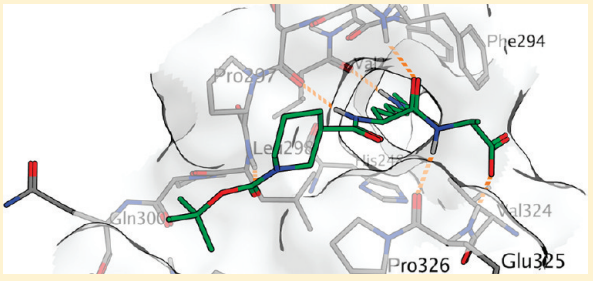

INTRODUCTION

The mammalian sirtuin family of class III deacetylases (SIRT1-SIRT7) catalyzes the nicotinamide adenine dinucleotide (NAD^+) dependent deacetylation of N^ϵ-acetyllysine residues in multiple protein substrates to nicotinamide, *O*′-acetyl-ADP-ribose (*O*AADPR) and N^ϵ-deacetylated lysine. The reversibility of the acetylation state of sirtuin target proteins by acetylases and deacetylases regulates diverse biological processes which have implications in devastating age-related diseases, such as cancer and metabolic, cardiovascular and neurodegenerative diseases.[1−4] Thus, it is important to discover small molecular regulators and to study sirtuin functions in cells. The most relevant therapeutic prospects for SIRT1 and SIRT2 inhibitors are for the treatment of cancer, either by inducing cell death or by preventing angiogenesis.[1,5−9] SIRT2 inhibitors have also been demonstrated to rescue proteotoxicity in neurodegenerative diseases.[10,11]

Several substrate based peptides have been reported to inhibit sirtuins. The inhibition was gained by replacing the acetyllysine with N^ϵ-thioacetyl-,[12−18] N^ϵ-selenoacetyl-,[17] N^ϵ-isovaleryl-,[17] N^ϵ-3,3-dimethylacryl-,[17] or N^ϵ-trifluoroacetyllysine.[14,19] However, apart from the acetyllysine analogue, the peptidic inhibitors can have various sequences (Figure 1),[16] which reflects the fact that sirtuins can deacetylate various substrates.[4] Recently, we demonstrated that a tripeptide is sufficient length for peptidic SIRT1 inhibitors and that an N^α-acetylated tripeptide has sufficient length for SIRT2 inhibition.[16,17]

In general, peptidic inhibitors may show advantages over small molecules in terms of specificity and affinity for different targets,[20] but unmodified peptides do not possess druglike properties; they are poorly bioavailable and vulnerable to nonspecific enzymatic degradation, which drastically limits their use as pharmacological tools. To move from peptidic toward small molecule inhibitors Suzuki et al. have recently presented a pseudopeptide backbone Cbz-Lys-NH-Ph with N^ϵ-3-ethoxy-3-oxopropanoyl[21] and the N^ϵ-thioacetyl[15] substitutions at the lysine side chain. Furthermore, the activity of the latter compound was demonstrated in cellular studies. Pseudopeptides have potential to overcome the aforementioned problems with peptides.

In order to develop potent pseudopeptidic inhibitors it is important to validate essential substrate−enzyme interactions, which may also define affinity of inhibitors. The available crystal structures are still limited, and for SIRT1 only a comparative model has been reported.[22] For SIRT2, the only reported crystal structure is in the apo form.[23] The fact that the substrate binding is associated with significant domain movements[24,25] compromises the value of the available SIRT2 and SIRT1 structures in the structure-based design of inhibitors.

Received: December 21, 2010
Published: September 07, 2011

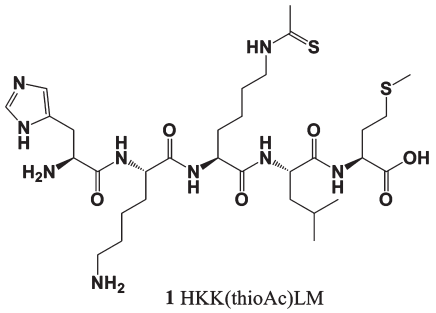

1 HKK(thioAc)LM

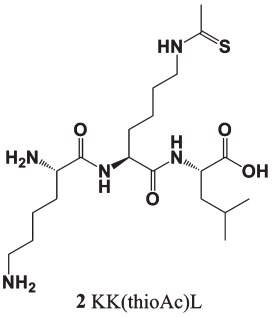

2 KK(thioAc)L

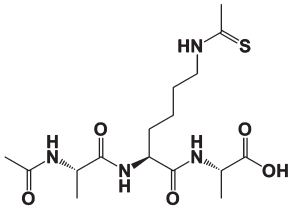

3 Ac-AK(thioAc)A

Figure 1. N^{ε}-Thioacetyllysine containing sirtuin inhibitors with various peptide sequences.

In this work, we aim to study whether SIRT3 could serve as a target structure in design, and help to screen scaffolds for pseudopeptidic inhibitors of SIRT1 and SIRT2. Based on the SIRT3 crystal structure, we have created a binding hypothesis for pseudopeptidic inhibitors. We have synthesized a series of pseudopeptidic SIRT1 and SIRT2 inhibitors and studied how they fulfill the binding hypothesis. The best inhibitors have comparable potency to the peptidic ones.

CHEMISTRY

Synthesis routes and reaction conditions are shown in Scheme 1. To obtain compound **8**, the amino terminal of N^{ε}-Cbz-Lys-OH was protected with a 9-fluorenylmethoxycarbonyl (Fmoc) group to give **4**. Compound **4** was taken to solid phase peptide synthesis (SPPS) on Wang resin and cleavage as a methyl ester with a mixture of MeOH, *N*,*N*-diisopropylethylamine (DIPEA) and *N*,*N*-dimethylformamide (DMF) gave **5**. The methyl ester was treated with methylamine (**6**), and the Cbz group was removed by hydrogenation on palladium (**7**). Finally, N^{ε}-thioacetylation of the free amine with ethyl dithioacetate gave compound **8**. Similarly, the N^{ε}-thioacetyl group was introduced to N^{α}-Fmoc-Lys-OH·HCl and N^{α}-Cbz-Lys-OH to gain compounds **12** and **26** respectively. Compounds **13**−**24** were synthesized with SPPS on Wang resin using appropriate carboxylic acids, *O*-(benzotriazol-1-yl)-*N*,*N*,*N*′,*N*′-tetramethyluronium tetrafluoroborate (TBTU) and DIPEA in the coupling phase and piperidine for the deprotection. Cleavage from the resin with 1 M NaOH (aq) in dioxane gave a free carboxylic acid, and cleavage with a mixture of MeOH, DIPEA and DMF gave a methyl ester. Compounds **27**−**30** were synthesized in solution phase using appropriate amine and TBTU as a coupling reagent. Reference compounds **1**, **2**, **3** and **25** were synthesized as described previously.[16,17]

RESULTS AND DISCUSSION

Peptidic Inhibitors. We have previously shown that pentapeptide HKK(thioAc)LM (**1**) and tripeptide KK(thioAc)L (**2**) give similar inhibitory activity against SIRT1 while compound **1** is a 24 times more potent SIRT2 inhibitor than compound **2**.[16] We have also shown that N^{α}-acetylated tripeptide Ac-AK(thioAc)A (**3**) gives good SIRT1 and SIRT2 inhibition.[17] In order to get a complete picture about the structure activity relationship (SAR) of peptidic inhibitors before the design of pseudopeptidic ones, we synthesized compounds **8** and **13**−**17** (Table 1).

The free carboxyl terminal of compound **3** was blocked as methyl amide (**8**) and as methyl ester (**13**). While SIRT1 slightly favored the free carboxyl terminal (**3**), SIRT2 inhibition was improved by the additional amide bond at the C-terminus (**8**). Methyl ester (**13**) with the least hydrogen bonding sites gave the weakest inhibition of SIRT1 and SIRT2.

Because N^{α}-acetylated tripeptide Ac-AK(thioAc)A (**3**) had turned out to be a surprisingly good SIRT2 inhibitor compared to tripeptide KK(thioAc)L (**2**),[16,17] we examined the inhibitory activity of tripeptide AK(thioAc)A (**14**). As expected, it was significantly more potent than compound **2** against SIRT2. This further reinforces the picture that no specific side chains are required for binding but, quite the contrary, some side chains can disrupt it. However, the N^{α}-acetylated **3** was more potent than compound **14**.

The K^{thioAc}+1 residue is known to be important for inhibitory activity.[16] We synthesized compounds **15** and **16** in order to study the role of the K^{thioAc}−1 residue in binding. Both compounds showed only weak or no inhibitory activity against SIRT1 and SIRT2 compared to compound **14**. It can be concluded that both residues flanking the thioacetyllysine are needed for binding.

In the available X-ray structures cocrystallized with a substrate peptide, the peptide backbone has a change in the orientation at the K^{Ac}−1 position (see for example Figure 3a), which may help to stabilize the substrate−protein interaction at the K^{Ac}−1 and K^{Ac}−2 sites. Compound **17** with a conformationally restricted Ac-Pro moiety at the N-terminal was found to be nearly equipotent with pentapeptide **1** and compound **3** for SIRT1, but slightly less potent for SIRT2. The slight preference for SIRT1 over SIRT2 makes the usage of proline a valid way to restrict conformational orientation of SIRT1 inhibitors.

Based on the peptidic inhibitors, it was concluded that (1) the amide bonds at both sides of the thioacetyllysine need to be preserved to ensure hydrogen bonding and proper orientation of the thioacetyllysine, (2) no side chains of amino acids need to be mimicked, and (3) in order to obtain SIRT2 inhibition, the pseudopeptides should stretch over larger area than tripeptides cover.

Substrate Binding Area and the Creation of the Binding Hypothesis. Although there are no substrate-bound structures for SIRT1 or SIRT2, the key interactions of the substrate−enzyme complex in the vicinity of the acetylated lysine residue are well-defined for example in the crystal structures for SIRT3 (PDB code 3glr)[24] and Sir2Tm (PDB code 2h2d)[25]

dx.doi.org/10.1021/jm200590k |*J. Med. Chem.* 2011, 54, 6456–6468

Scheme 1[a]

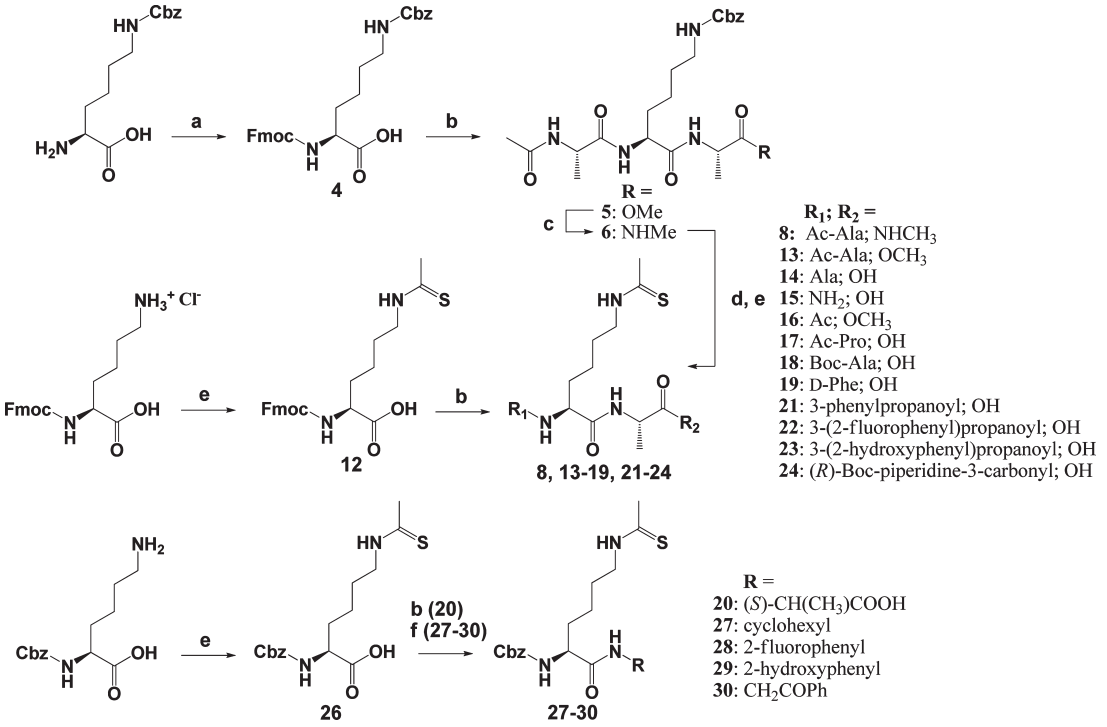

[a] Reagents and conditions: (a) 9-fluorenylmethyl chloroformate, 0 °C to rt, 4 h; (b) solid phase peptide synthesis with Fmoc strategy [(coupling) appropriate carboxylic acid, TBTU, DIPEA, DFM, rt, 1 h; (Fmoc deprotection) 20% piperidine/DMF; (cleavage as −COOH) 1 M NaOH (aq) / dioxane (2:6), rt, 1 h, filtration, 3 M HCl (aq) or (cleavage as $-COOCH_3$) DIPEA/MeOH/DMF (1:5:5), heat at reflux, overnight]; (c) 8 M methylamine in EtOH, 100 °C, 20 min; (d) 10% Pd on charcoal, MeOH, rt, overnight; (e) ethyl dithioacetate, EtOH/10% (w/v) Na_2CO_3 (aq) (3:1), rt, 12−48 h; (f) appropriate amine, TBTU, DMF/pyridine (1:1), 0 °C to rt, 1−2 h.

Table 1. SIRT1 and SIRT2 Inhibitory Activities of the Peptidic Inhibitors

compd		IC_{50}[a] (μM)	
		SIRT1	SIRT2
1[13,16]	HKK(thioAc)LM	0.31 (0.27−0.36)	6.3 (5.5−7.2)
2[16]	KK(thioAc)L	0.57 (0.38−0.84)	151 (104−218)
3[17]	Ac-AK(thioAc)A	0.24 (0.20−0.28)	9.8 (8.7−11)
8	Ac-AK(thioAc)A-NHMe	0.40 (0.35−0.46)	2.9 (2.6−3.3)
13	Ac-AK(thioAc)A-OMe	1.0 (0.82−1.3)	13 (9.5−19)
14	AK(thioAc)A	0.66 (0.60−0.74)	36 (29−46)
15	K(thioAc)A	nd[b]	nd[c]
16	Ac-K(thioAc)A-OMe	51 (37−68)	862 (417−1782)
17	Ac-PK(thioAc)A	0.37 (0.35−0.39)	31 (28−33)

[a] Fluor de Lys based assay (repeated at least three times, 95% confidence intervals in parentheses). [b] IC_{50} was not determined. Inhibition % at 200 μM ± standard deviation (n = 2−3) was 46.9 ± 3.0%. [c] IC_{50} was not determined. Inhibition % at 200 μM ± standard deviation (n = 2−3) was 2 ± 0.9%.

(Figures 2a and 2b, respectively). In the SIRT3 structure the reactive acetyllysine of the substrate is located in a tunnel shaped groove formed between the Rossman fold and the zinc binding domains. The substrate binding has been claimed to induce movement of the two domains relative to each other, which significantly reduces the size of the cavity of the acetyllysine binding site.[25] The orientation of the substrate backbone is dictated by a hydrogen bond network between the substrate main chain and the backbone of protein residues Gly295, Glu296, Glu323 and Glu325 (SIRT3 numbering) (Figure 2a). The reactive acetyllysine is oriented toward the NAD^+ binding site by a hydrogen bond of the acetyl carbonyl with Val292. In addition, at the $K^{Ac}-2$ position, the substrate potentially has a water molecule mediated hydrogen bond with Leu298.

Comparison of the SIRT3 structure to the crystal structure of the Sir2Tm substrate complex (PDB code 2h2d)[25] (Figure 2b) indicates that small differences in the binding site sequences (Figure 2c) do not lead to any significant changes in the substrate binding orientations. The interaction pattern between substrates and proteins is similar in SIRT3 and Sir2Tm structures, and consists mainly of main chain interactions. It is assumed that this can be generalized to the active sites of SIRT1 and SIRT2.

Substrate-bound SIRT3 (PDB code 3glr) was used as a target structure to study the substrate binding area. Based on the peptide modifications and substrate-bound crystal structures, it was obvious that only main chain interactions were critical for the substrate binding. However, we wanted to get a more detailed insight on the substrate binding site in order to design potent pseudopeptidic inhibitors for sirtuins. Two virtual libraries of various possible pseudopeptides were created by attaching various chemical structures to the terminals of a thioacetyllysine amino acid. The libraries were docked in the crystal structure of SIRT3 to study the chemical space of molecules that can be docked to the substrate binding site allowing the thioacetyllysine to be placed similarly as the acetyllysine in the X-ray structure. A binding hypothesis for pseudopeptidic inhibitors was generated based on the docking results (Figure 3a−e).

dx.doi.org/10.1021/jm200590k | J. Med. Chem. 2011, 54, 6456–6468

Interaction Criteria Proposed by the Binding Hypothesis. Hydrogen bonds observed from the acetylated lysine in the SIRT3 crystal structure to Val292, Gly295, Glu296 and Glu325 were assumed to be vital for the proper orientation of the acetylated lysine (Figures 3a and 3b). A change in the substrate peptide backbone orientation is seen at the $K^{Ac}-1$ glycine residue position (Figure 3a). This change in the orientation places the backbone to a crevice between residues Pro297 and Pro326. The crevice between residues Pro297 and Pro326 leads to a small cavity formed by residues Pro297, Leu298, Gln300, Phe302 and Leu303 (Figure 3c). It was hypothesized that binding affinity could possibly be increased by occupying the cavity with an appropriate structure and that Leu298 could offer an additional hydrogen bonding site (Figure 3c), although the substrate peptide in the crystal structure did not form a direct hydrogen bond at this location. On the C-terminal side, it was noted that the location of the amino acid Phe294 could offer a possibility for aromatic interactions (Figure 3d,e). In addition, the backbone amine of Glu325 could serve as an additional hydrogen bonding partner.

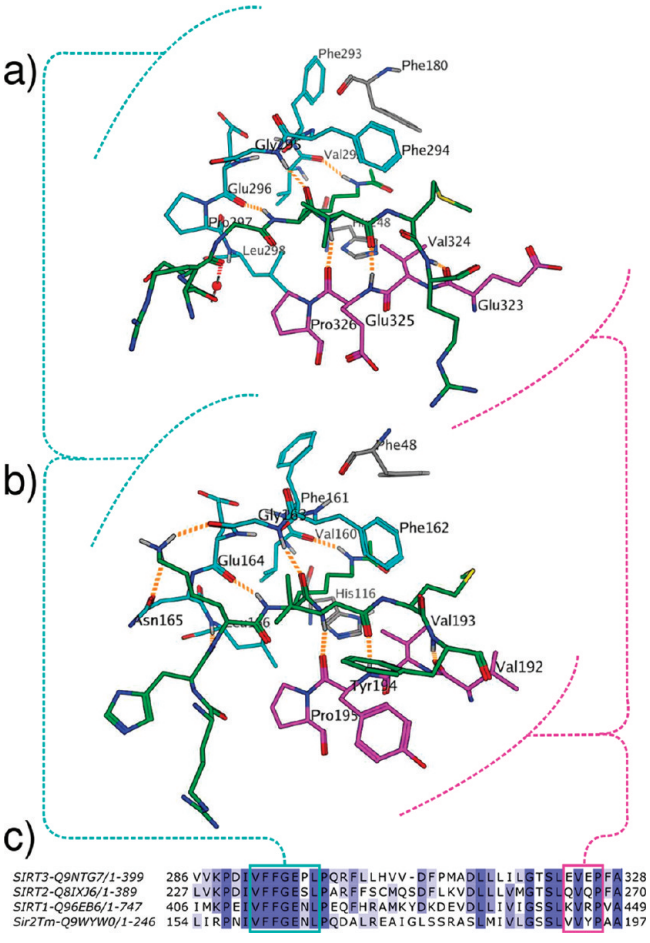

Figure 2. Crystal structures of (a) SIRT3 (PDB code 3glr)[24] and (b) Sir2Tm (PDB code 2h2d)[25] showing the substrate binding site around the acetylated lysine. (c) The sequence homology of SIRT1−3 and Sir2Tm in the binding site area.

Analysis of the in Vitro Results in Light of Molecular Docking. A series of pseudopeptides was designed (Table 2). The first group of compounds has L-alanine at the C-terminal site of the thioacetyllysine residue and various N-terminal modifications. The second group has the benzyloxycarbonyl group at the N-terminal site of the thioacetyllysine residue and various C-terminal modifications. The N- and C-terminal modifications consist of non-natural peptidic fragments (**18**, **19**), known structures and their modifications (**20**, **21**, **25**, **27**), structures with different H-bonding properties (**22**, **23**, **28**, **29**) and structures from the virtual libraries selected based on the binding hypothesis (**24**, **30**).

The docking poses are presented in Figure 4 (see Figure S1 in the Supporting Information for additional figures). The Glide scores (Table 3) represent the overall docking score, while the per-residue scores are listed to present hydrogen bond patterns of the docking poses. The root-mean-square deviation (rmsd) value represents the similarity of the thioacetylated lysine poses of the docked compounds to the cocrystallized acetylated lysine (PDB 3glr). The in vitro inhibitory activities are presented in Table 2.

Compounds **18** and **24** have the Boc-L-alanine and Boc-piperidine-3-carbonyl fragments at the N-terminus, respectively.

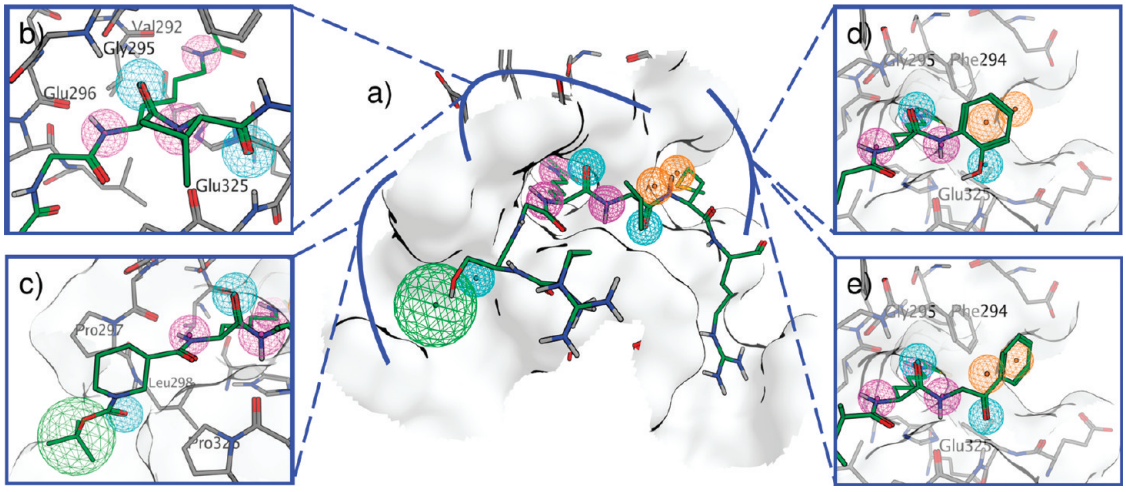

Figure 3. The binding hypothesis represented with wire spheres for pseudopeptidic inhibitors. (a) The molecular structure (green carbon atoms) represents the binding mode of the peptide cocrystallized with SIRT3 (PDB 3glr). (b) The key hydrogen bonds formed by the acetylated lysine in the SIRT3 (blue and magenta spheres). (c) N-Terminal modification from the virtual database screening that forms a hydrogen bond to Leu298 (blue sphere) and fills a cavity surrounded by residues Pro297, Leu298, Phe302 and Leu303 (green sphere). (d, e) Possibility for aromatic interactions found from the virtual database screening (orange spheres).

dx.doi.org/10.1021/jm200590k |J. Med. Chem. 2011, 54, 6456–6468

Table 2. The Studied N- and C-Terminal Fragments and in Vitro Inhibitory Activities of the Synthesized Compounds

Compd	R	SIRT1 IC_{50} (μM)[a]	SIRT2 IC_{50} (μM)[a]	HDAC % Inhibition ± SD at 200 μM
	R-NH-K(thioAc)-Ala-OH			
18	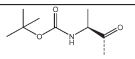	0.77 (0.66-0.89)	6.5 (5.9-7.2)	10.1 ± 5.8
19	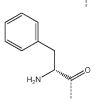	18 (14-23)	N.D.[b]	7.6 ± 1.6
20	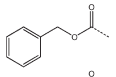	1.3 (1.1-1.5)	17 (14-22)	3.9 ± 0.4
21	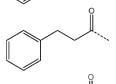	0.99 (0.76-1.29)	56 (42-73)	8.5 ± 0.5
22	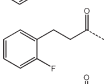	1.3 (1.1-1.5)	27 (18-41)	16.3 ± 0.6
23	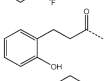	1.0 (0.9-1.1)	53 (46-58)	5.6 ± 0.1
24	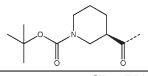	0.97 (0.87-1.1)	13 (12-15)	23.7 ± 1.4
	Cbz-K(thioAc)-NH-R			
25[15, 17]		9.9 (8.3-12)	15 (13-17)	2.5 ± 0.2
27		23 (18-28)	N.D.[c]	75.4 ± 2.2
28		7.4 (6.4-8.4)	16 (12-21)	1.4 ± 1.2
29		5.1 (4.6-5.7)	7.4 (5.6-9.9)	1.9 ± 1.7
30		1.6 (1.4-1.8)	4.3 (3.5-5.3)	5.1 ± 0.2

[a] Fluor de Lys based assay (repeated at least three times, 95% confidence intervals in parentheses). [b] IC_{50} was not determined. Inhibition % at 200 μM ± standard deviation (n = 2−3) was 22.4 ± 3.0. [c] IC_{50} was not determined. Inhibition % at 200 μM ± standard deviation (n = 2−3) was 57.2 ± 1.4.

The Boc-piperidine-3-carbonyl fragment was chosen among the fragments in the previously created virtual libraries and was used in the formation of the binding hypothesis (Figure 3c). Compounds **18** and **24** were synthesized to test the hypothesis that the shape of the receptor surface on the N-terminal side allows the size of the N-terminal modification to be increased. The docking poses of these compounds showed the N-terminal fragment binding through the crevice, placing the *tert*-butyl moiety in the small cavity and the carbamate carbonyl H-bonded with Leu298 (Figure 4a and Table 3). Thus, these compounds fulfilled all the N-terminal binding criteria proposed by the binding hypothesis and are the two most potent compounds in the series of the N-terminal modifications. Compared to Ac-AK(thioAc)A peptide (**3**), compounds **18** and **24** showed equipotent SIRT2 inhibitory activity and slightly reduced SIRT1 inhibitory activity. For complementary binders, the increase in size usually increases the inhibitory activity; therefore, it may be that the binding conformation of compounds **18** and **24** is not optimal for SIRT1 and SIRT2.

One D-amino acid was chosen into the set of N-terminal modifications. D-Phenylalanine in compound **19** has two atoms between the phenyl and carbonyl groups as has the Cbz group, a known N-terminal fragment.[15] In the docking calculations the free amino terminal of the D-phenylalanine showed H-bonding to Gly295 but the phenyl group was not placed in the crevice between Pro297 and Pro326 and no hydrogen bonding to Leu298 was formed (see Figure S1 in the Supporting Information). This compound did not fulfill any of the criteria proposed by the binding hypothesis, and it is also the least active compound in the series of N-terminal modifications. The additional H-bond to Gly295 seen in the docking to SIRT3 does not correlate well with the inhibitory activity toward SIRT1 or SIRT2.

Table 3. The Glide Docking Results of the Pseudopeptide Compounds

compd	Glide gscore	Glu325 hbond	Leu298 hbond	Glu296 hbond	Gly295 hbond	Val292 hbond	subset rmsd[a]
18	−8.85	−1.50	−0.72	−1.00	−0.94	−1.00	0.28
19	−8.06	−1.50	0.00	−1.00	−0.96	−1.00	0.82
20	−8.47	−1.50	0.00	−1.00	−1.00	−1.00	0.26
21	−8.41	−1.50	0.00	−1.00	−0.85	−1.00	0.42
22	−8.66	−1.50	0.00	−1.00	−0.96	−1.00	0.29
23	−8.81	−1.50	0.00	−1.00	−2.00	−1.00	0.63
24	−9.71	−1.50	−1.00	−1.00	−1.00	−1.00	0.29
25	−8.00	−1.00	0.00	−1.00	−1.00	−1.00	0.26
27	−8.00	−1.00	0.00	−1.00	−0.96	−1.00	0.27
28	−8.28	−1.00	0.00	−1.00	−1.00	−1.00	0.24
29	−8.60	−2.00	0.00	−1.00	−1.00	−1.00	0.27
30	−8.97	−2.00	0.00	−1.00	−1.00	−1.00	0.62

[a] Rmsd calculated between the common core substructure of the compounds and the substrate peptide. The common core structure was defined by the SMARTS pattern C(=O)NC(CCCCNCC)(C(=O)N).

In order to gain more insight into the effect of modifications in the N-terminal, docking studies were carried out for compounds **20**−**23**. The N-terminal Cbz group (**20**) has been presented by Suzuki et al.[15] In compound **21**, the Cbz group was replaced by the 3-phenylpropanoyl group. This modification was made in order to study whether the removal of the oxygen in the chain affects the activity. Docking calculations did not show any significant differences in the binding of these compounds, and the N-terminal structures were well superimposed (Figure 4b). Both compounds bind to the crevice but do not reach all the way to the cavity and do not form an H-bond to Leu298 thus fulfilling one of the three binding criteria. The rmsd values illustrating the similarity of the lysine orientation were small for both compounds (Table 3). Compared to compound **20**, compound **21** had equipotent SIRT1 but slightly decreased SIRT2 inhibitory activity. This decrease in the activity cannot be explained by docking to SIRT3.

Compound **21** was further modified by additional hydrogen bonding groups (**22** and **23**). The position of the phenyl group of compound **22** is slightly different compared to compound **21** but is still positioned to the crevice (Figure 4c). The placement of fluorine could allow H-bonding to Leu298, but the GlideScore scoring function does not consider fluorine as a hydrogen bond acceptor. The SIRT1 in vitro results do not support Leu298 H-bonding, but in the case of SIRT2 it cannot be excluded. The docking pose of compound **23** to the SIRT3 is different compared to compound **21** (Figure 4c). The phenyl group is

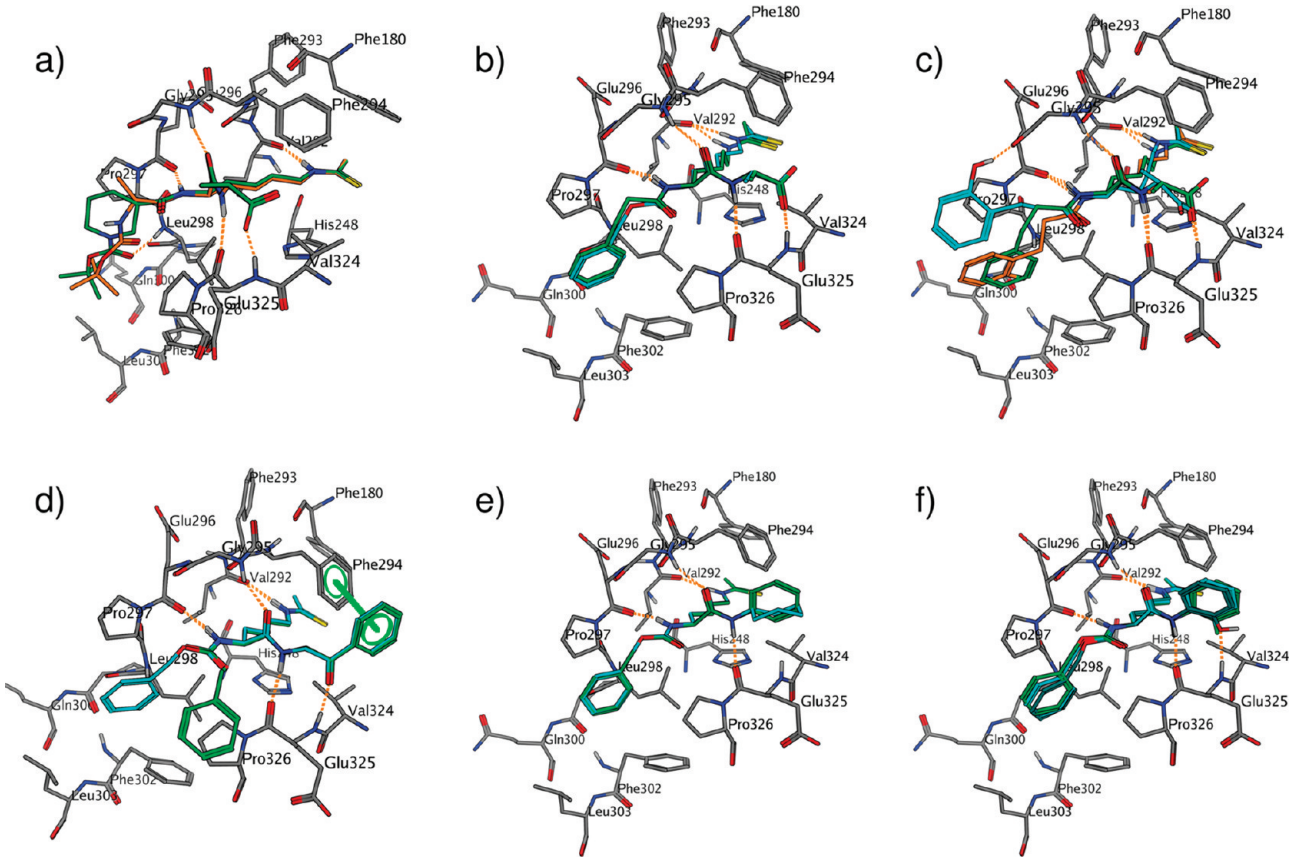

Figure 4. The docking poses of the pseudopeptides. The interactions were predicted with the Ligand Interactions tool available in MOE.[26] (a) The docking poses of compounds **18** and **24** showed binding to the crevice between Pro297 and Pro326, positioning of the *tert*-butyl groups in a pocket surrounded by residues Pro297, Leu298, Gln300, Phe302 and Leu303 and hydrogen bonding to Leu298. (b) The docking poses of compounds **20** (cyan) and **21** (green). (c) The docking poses of compounds **22** (orange) and **23** (cyan) compared to compound **21** (green). Compound **23** was hydrogen bonded to Gly295. (d) The docking pose of compound **30** showing aromatic interactions with Phe294 and hydrogen bonding to Glu325. The best ranked pose (green) had the N-terminal amide in the *cis*-form while the second ranked pose (cyan) had the N-terminal amide in the *trans*-form. However, the poses of the C-terminal fragment were identical. (e) The docking poses of compounds **25** (green) and **27** (cyan) placed the cyclohexyl and phenyl moieties in the same location. (f) The docking poses of compounds **25** (green), **28** (cyan) and **29** (dark cyan) with the overlaid phenyl moieties. The hydrogen bond acceptors hydroxyl and fluorine are toward the backbone amine of Glu325.

not positioned to the crevice, and the hydroxyl group forms an H-bond to Gly295. However, the in vitro results are similar for these compounds and, again, the additional hydrogen bond to Gly295 found in the pose is not supported by the in vitro activities. It is possible that the docking pose of **23** to SIRT3 may not represent the binding to SIRT1 or SIRT2.

The C-terminal modification in compound **30** was chosen among the fragments in the previously created virtual libraries and was used in the creation of the binding hypothesis (Figure 3e). The docking pose of compound **30** (Figure 4d) positions the ketone carbonyl to form a hydrogen bond to Glu325. When the pose was analyzed with the Ligand Interaction tool of MOE (version 2009.10),[26] the adjacent phenyl ring was predicted to have aromatic interactions with Phe294. This compound fulfills both binding criteria for the C-terminal binding proposed by the binding hypothesis and is the most potent compound in the series of C-terminal modifications.

When the previously published compound **25**[15,17] is compared to compound **30**, it is seen that the phenyl group is positioned differently (Figure 4e). Compound **25** also lacks the H-bond to Glu325. The differences in the docking poses are reflected by the in vitro inhibitory activities; compound **30** was more potent than compound **25** against both enzymes. The Ligand Interaction tool of MOE did not detect aromatic interactions between the phenyl ring of **25** and Phe294. However, when the phenyl group was replaced by a cyclohexyl group (**27**), the inhibitory activity against SIRT1 and SIRT2 decreased. This proved the importance of the phenyl group even though the docking scores and the per-residue hydrogen bonding scores were nearly equal for these compounds (Table 3 and Figure 4e). It may be that the receptor flexibility allows aromatic interactions of the phenyl group with Phe294 although the interaction may not be as optimal as for compound **30**. However, compound **27** with the cyclohexyl group at the C-terminus does not fulfill the criteria of the aromatic interactions or the H-bond to Glu325 and is the least active compound in the series.

Compounds **28** and **29** are derivatives of compound **25** with an additional hydrogen bonding group. The docking poses of compounds **25**, **28** and **29** were well superimposed (Figure 4f). The C-terminal phenyl group of all three compounds had similar position and orientation. The position of the hydroxyl oxygen of compound **29** allowed hydrogen bond formation to residue Glu325, and slight improvement is also seen in the inhibitory activities. The fluorine of compound **28** is also in a position that

dx.doi.org/10.1021/jm200590k |*J. Med. Chem.* 2011, 54, 6456–6468

Table 4. The Number of Successfully Docked Compounds on Various SIRT3, SIRT2 and Sir2Tm Crystal Structures and SIRT1 and SIRT2 Models[a]

PDB code	protein	cocrystallized substrate	no. of successfully docked compounds
3glr	SIRT3	AceCS2-K^{Ac}	18/20
3gls	SIRT3	apo	0/20
3glt	SIRT3	AceCS2-K^{Ac}-ADPR	13/20
3glu	SIRT3	AceCS2	18/20
1j8f	SIRT2	apo	0/20
2h2d	Sir2Tm	p53-$K382^{Ac}$	19/20
2h2f	Sir2Tm	p53-K382	19/20
2h2g	Sir2Tm	H3-$K115^{Ac}$	18/20
2h2h	Sir2Tm	H4-$K79^{Ac}$	18/20
2h2i	Sir2Tm	apo	0/20
model	SIRT1		18/20
model	SIRT2		8/20

[a] In order to be considered as a successful docking pose, the thioacetyllysine had to form the three hydrogen bonds seen in substrate-bound sirtuin structures (e.g. PDB code 3glr).

allows hydrogen bonding to the backbone amine of Glu325, but no effect on the inhibitory activities was observed. No hydrogen bonding scores were seen, either, in the per-residue scores (Table 3), but this is because the GlideScore scoring function does not consider fluorine as a hydrogen bond acceptor.

The binding hypothesis created by using SIRT3 structure seems to predict quite well binding to SIRT1 and SIRT2 although there are some reservations. The most active N- and C-terminal modifications (**18**, **24** and **30**) fulfilled all the binding criteria proposed by the hypothesis while the least active modifications (**19** and **27**) failed to fulfill them. On the N-terminal side, the occupation of the cavity seemed to be important for SIRT2 while SIRT1 can be inhibited with shorter compounds. This is well in line with the SAR of the peptidic inhibitors. Hydrogen bonding to Leu298 in the SIRT3 structure does not seem to correlate with SIRT1 in vitro activity, while some correlation in the case of SIRT2 was seen. The proposed hydrogen bonding of compounds **19** and **23** to Gly295 was not supported by the in vitro results. On the C-terminal side, both the hydrogen bonding to Glu325 and the aromatic interactions with Phe294 in the SIRT3 structure predicted good inhibitory activities for SIRT1 and SIRT2 inhibitors. The proposed binding hypothesis can be used in the design of SIRT1 and SIRT2 inhibitors although all affinity differences between these two targets cannot be explained. This would require detailed structural data on the SIRT1 and SIRT2 substrate binding sites in the substrate binding conformation, but because of the lack of crystal structures, this data is not available.

There are 11 globular isoforms of human histone deacetylases (HDACs) with conical pockets that fit acetylated lysine residues. The pseudopeptidic compounds were tested on a mixture of class I and class II HDACs to study inhibition among HDACs. The compounds did not show high inhibition activities in the HDAC assay (Table 2). Compound **27** was the only compound that showed some response.

Sensitivity of the Modeling Approach To Target Protein Differences. In order to test how sensitive the used molecular docking approach is to sequence differences, the synthesized compounds (excluding compound **2**) were docked again to several sirtuin X-ray structures and two homology models representing different conformational forms. These structures included four different SIRT3 X-ray structures, one SIRT2 X-ray structure, one SIRT2 homology model, one SIRT1 homology model and five Sir2Tm structures. The homology models of SIRT1 and SIRT2 were based on the substrate binding X-ray structures of SIRT3. The target set included one apo structure from each protein.

The resulting docking poses were visually analyzed to see whether the synthesized compounds fulfill the hydrogen bonding network of the thioacetyllysine (see Figures S2−S13 in the Supporting Information for the docking poses). The docking results are presented in Table 4. The results of SIRT3, Sir2Tm and SIRT1 calculations indicated that the obtained docking poses are not sensitive to small sequence differences. The compounds could be docked into correct docking poses with a high success rate on all of these proteins. However, the protein conformation seemed to have a bigger effect on the docking results. Dependence of the success rate on the conformation variation was observed on SIRT3 and Sir2Tm proteins. When the apo conformations of SIRT3, SIRT2, and Sir2Tm were used as the docking targets, none of the docked compounds resulted in a correct pose. This can be explained by the significant conformation difference and enlargement of the binding site cavity, caused by the movement of the two large domains.[25] The success rate was increased on SIRT2 when the homology model was used. However, a lower success rate was obtained with the SIRT2 model than with the SIRT1 model. The results do not explain whether the lower success rate is caused by sequence differences or by not optimally placed side chains of the SIRT2 model.

The results of this analysis gave further justification for our choice to use the SIRT3 crystal structure complexed with AceCS2-K^{Ac} substrate. As the small sequence differences in the substrate binding site did not seem to affect significantly the docking poses, the results can be postulated to give a somewhat reasonable prediction on the binding poses also on SIRT1 and SIRT2. The in vitro results supported these assumptions as several new active inhibitors were discovered in the process.

Inhibition of SIRT1 Activity in Cell Culture Models. To examine if the compounds are also active at the cellular level, we used Western blot analysis to detect the changes in acetylation level of p53 after etoposide-induced DNA damage in three different cell types. SIRT1 is known to be involved in deacetylation of p53 at those conditions.[15,27] The effect of compounds **20**, **24** and **30** on p53 acetylation rate in cells (Figure 5) is in accordance with the in vitro inhibition profile of SIRT1. Those compounds were not toxic to cells at concentrations used (data not shown).

CONCLUSIONS

Structure-based computational design approach was successfully applied in the design of N^{ε}-thioacetyllysine containing pseudopeptidic inhibitors of SIRT1 and SIRT2. Several designed pseudopeptidic inhibitors maintained the potency comparable to the peptidic inhibitors. Those N- and C-terminal fragments which gave the best inhibitory activities were the same fragments that fulfilled all the interaction criteria proposed by the binding hypothesis. On the other hand, those fragments which did not fulfill the set criteria gave the least active compounds. The pseudopeptides were shown to inhibit class III HDACs (SIRT1 and SIRT2), however no high inhibition responses were

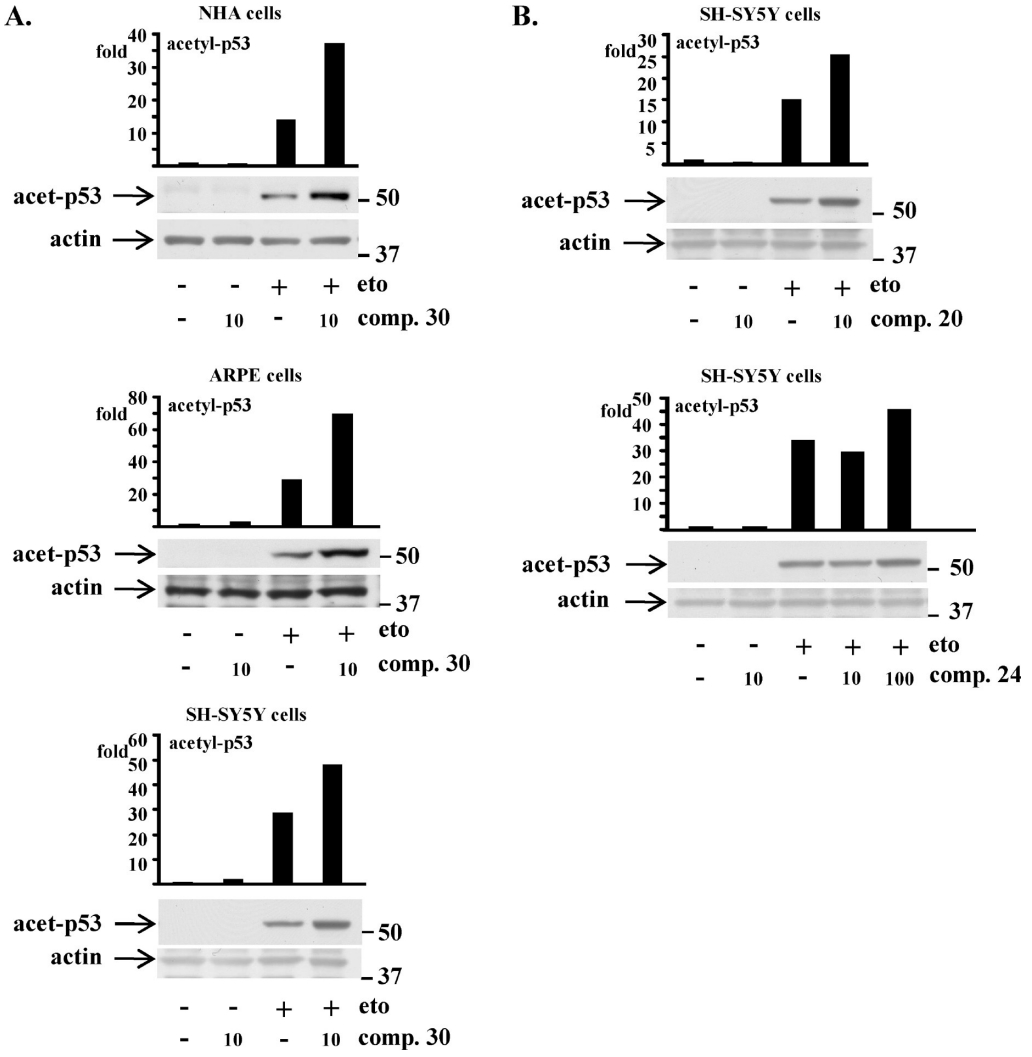

Figure 5. Inhibition of SIRT1 activity increases p53 acetylation after DNA damage. (A) Effect of 10 μM compound **30** on p53 acetylation after 100 μM etoposide (eto) treatment for 5 h in three different cell lines. (B) Effect of 10 μM compound **20** and 10 or 100 μM compound **24** on p53 acetylation after 100 μM etoposide treatment for 5 h in SH-SY5Y cells. + present; − absent.

observed in an assay that contained a mixture of class I and class II HDACs. Compounds **20**, **24** and **30** demonstrated SIRT1 inhibition also in cultured cells. It was concluded that the homologous SIRT3 structure can be used for designing substrate based inhibitors of SIRT1 and SIRT2. On the other hand, the available experimental SIRT2 structure in the apo conformation is not suitable for the design of substrate based modulators as the sirtuins undergo significant conformational changes upon substrate binding.[25]

EXPERIMENTAL SECTION

The Virtual Databases. The first virtual database was created using the RECAP synthesis tool of MOE (Molecular Operating Environment) version 2008.10.[26] The thioacetyllysine structure was used as a root structure in the RECAP synthesis process, and molecular fragments were attached to both terminals of the thioacetyllysine. The fragments were taken from a small-size fragment subset of the RECAP fragment database provided with MOE. The subset contained all fragments of size 12 or less heavy atoms from the MOE RECAP database. The RECAP synthesis process was run with default settings except the size limit was increased to 35 heavy atoms with default value of 11 for the standard deviation setting. The Leadlike filter was left on, and no exclusion for the reactive compounds was done. The RECAP synthesis was set to continue until 10000 compounds or 1000000 repeated attempts had been performed. The thioacetyllysine structure was set as a root structure by placing the structure in a MOE database and by forcing the root structure to be always selected from this database. The weight setting, which defines the probability that a fragment is selected from this database, was set to 0 for the root database and 1 for the small size fragment database, forcing the fragments to be selected from the latter. Overall 10000 structures were generated. Hydrogens were added to the created molecules using the Database Wash function in MOE. Prior to subjecting the ligands to docking, the compounds were preprocessed with Ligprep (version 2.3).[28] The molecules were imported to Ligprep in sdf format. The ionization and tautomeric states were determined with EPIK[29] (version 2.0) in pH of 7 ± 2. OPLS2005 force field was used for the geometric optimization.

The second virtual database was created using CombiGlide (version 2.5).[30] The fragment ideas were obtained from a list of selected structure sets available from the chemical vendor Sigma-Aldrich. The carboxylic acid containing fragments were downloaded in sdf format from the Sigma-Aldrich web page (http://www.sigmaaldrich.com/chemistry/chemistry-services/selected-structure.html, accessed January 27th, 2010).

The carboxylic acid fragments were prepared with the Reagent Preparation process of CombiGlide. The carboxylic acid group was defined as the reactive functional group. No changes to the ionization, tautomerization and steroisomer states of the fragments were made at this point. Thioacetyllysine−alanine structure, used as a core structure in the CombiGlide process, was built and energy minimized in MOE (version 2009.10)[26] and later prepared with Ligprep (version 2.3)[28] using OPLS2005 forcefield for geometric optimization. The fragments were attached to the N-terminal of the core structure using the Combinatorial Library Enumeration tool of CombiGlide. Overall 6748 structures were generated. Prior to subjecting the structures to docking they were prepared with Ligprep. OPLS2005 force field was used for geometric optimization, all possible protonation and tautomeric states were generated with EPIK at pH 7 ± 2 and chiralities if defined were taken from the 3D structure.

The Docking Calculations. The docking calculations were performed using Glide (version 5.5)[31] molecular docking program. The X-ray crystal structure of human SIRT3 protein complexed with an acetylated lysine structure (PDB code 3glr)[24] was used as a target in the docking calculations performed on the virtual databases. The protein structure was prepared using the Protein Preparation Wizard available in the Schrödinger Suite 2009.[32] The PDB structure was downloaded from www.rcsb.org using the Import command of the Protein Preparation Wizard (PDB download date December 18th, 2009). In the preprocess phase of the Protein Preparation Wizard the bond orders were assigned, hydrogens were added, distant water molecules were removed, metals were treated and overlaps were detected. Later all water molecules and HET groups except the zinc were removed. Exhaustive sampling method was used to optimize the hydrogen bonding and determine the orientations of hydroxyl groups, amide groups of Asn and Gln amino acids, and the proper state and orientations of the histidine imidazole rings. Finally a restrained minimization was performed using OPLS2001 force field, with a 0.3 Å rmsd atom displacement limit.

The prepared protein structure was used in the receptor grid generation process. The acetyllysine containing peptide was defined as a ligand to be excluded, and the peptide defined the grid box location and the size of the outer box. Default values were used for all the other available options and settings for the grid calculations.

The same receptor grid files were used in the docking calculations of both virtual databases. The dockings were performed using the SP (standard precision) precision option. The compounds were docked flexibly using the options that allow the algorithm to sample ring conformations but penalize the nonplanar amide bond torsion angles. 50 poses of each docked compound were subjected to post docking minimization. The other options and settings were left at their default values.

The synthesized and tested pseudopeptides were subjected to docking calculations. The molecular structures were exported in sdf format from a ChemBioOffice[33] database and prepared using Ligprep (version 2.3).[28] OPLS2005 force field was used for geometric optimization, and all possible ionization and tautomeric forms were created at pH 7 ± 2 using EPIK.[29] The chiralities specified in the input structures were retained. The same grid files were used in the dockings as in the virtual library dockings. The dockings were performed using the SP precision settings treating the compounds as flexible. The ring conformations were allowed to be sampled and nonplanar amide bond torsions penalized to favor planar conformations. 50 poses of each ligand were subjected to postdocking minimization, and an option for adding a strain correction term if the strain crossed the default strain limit was set on. The best ranked pose of each docked ligand was included in the analysis.

In order to test whether the docking results can be somewhat generalized to other sirtuin structures with differences in the conformations and in the amino acid sequences, the 20 different tested compounds (**1**, **3**, **8**, **13**−**25** and **27**−**30**) were docked to 4 human SIRT3 X-ray structures (PDB codes: 3glr, 3gls, 3glt and 3glu),[24] to 5 Sir2Tm X-ray structures (PDB codes: 2h2d, 2h2f, 2h2g, 2h2h and 2h2i),[25] to the only available SIRT2 X-ray crystal structure (PDB code 1j8f)[23] (the PDB files were downloaded between June 1 and June 3, 2010) and to homology models of SIRT1 and SIRT2. The homology models were built using MODELER in Discover Studio.[34] The templates used for the homology models were the crystal structure of SIRT3 with substrate (PDB codes: 3glr, 3glt and 3glu). Several models were generated, and side chains were optimized. The model with the smallest rmsd compared to 3glr was chosen for dockings. The protein structures were prepared with Schrödinger Suite 2009 (Update 2) Protein Preparation Wizard[32] in a similar automated fashion that was used for preparing the protein used in the virtual database dockings. The ligands were treated with Ligprep (version 2.3)[28] as described earlier. The grid box center for SIRT3 proteins was defined based on the amino acids Pro297, Pro326 and Phe294 for SIRT3 structures. Also the dockings for the 3glr crystal structure were repeated using the same grid box center in order to improve the comparability of the docking results. The corresponding amino acids were also used for defining the grid box center on the Sir2Tm, SIRT1 and SIRT2 proteins. The dockings were performed with the same Glide settings as the earlier dockings.

Result Analysis and Figure Preparation. The figures of the crystal structures 3glr and 2h2d (Figure 2) were prepared using MOE (version 2009.10).[26] Prior to the figure preparation, the structures were treated using the Protein Preparation Wizard (Schrödinger Suite 2009 Update 2).[32] This included bond order assignment, addition of hydrogens, removal of water molecules and heteroatomic groups. For the SIRT3 structure a water molecule close to amino acid Leu298 was not removed, and the zinc atoms for both structures were left untouched. The Ligand Interactions tool in MOE was used for predicting the interactions between the substrate peptides and their protein counterparts. The protein sequences for the sequence alignment were obtained from the UniprotKB[35] database (access date July 8, 2010). The sequence alignment was made with the online Clustalw2 (version 2.0.12)[36] alignment tool available at the UniprotKB web page. The alignment figure was prepared using Jalview (version 2.5.1).[37] The graphical effects on the final figure were prepared with Inkscape (version 0.47).

The binding mode hypothesis figure (Figure 3) was prepared using MOE (version 2009.10).[26] The protein structure in the figure is the one used in the virtual database screening. MOE pharmacophore annotations were used for describing the hypothesized interactions. The graphical effects on the figure were prepared using Gimp version 2.2.13 and ImageMagick version 6.5.1−0.

The figures describing the docking poses (Figure 4) were prepared using MOE (version 2009.10).[26] The interactions in the figures including the hydrogen bond possibilities and aromatic interactions were analyzed and visualized using the Ligand Interaction module available in MOE. The score limit for presenting a hydrogen bond was set to 10%. The figure labels were added with ImageMagick version 6.5.1−0.

Hydrogen bond scoring of Table 3 is based on the per-residue interaction scoring output of Glide. The rmsd value of Table 3 is a rmsd between a common substructure of the peptide substrate of the crystal structure 3glr and the synthesized ligands, defined with a SMARTS pattern C(=O)NC(CCCCNCC)(C(=O)N). The rmsd calculation was performed with a Schrödinger script rmsd.py (version 1.14.2.6)[38] downloaded from the Schrodinger Script Center Web site (http://www.schrodinger.com/scriptcenter, access date June 23th, 2010).

Chemistry. All reagents and solvents were commercial high purity quality. Purification of products **8**, **13**, **16**−**18**, **20**−**24** and **27**−**30** was performed by CombiFlash column chromatography on normal phase silica (average particle size, 35 to 70 μm; mesh, 230 to 400; average pore size, 60 Å) or by crystallization methods. Compounds **14**, **15** and **19** were purified by preparative HPLC (Shimadzu LC-10Avp (Shimadzu, Kyoto, Japan)) on a reverse phase C18 column (Supelcogel ODP-50, 25 cm × 21.2 mm, 5 μm) with a linear gradient of 5−90% solvent

B (0.05%acetic acid/acetonitrile) in solvent A (0.05 acetic acid/H_2O) in 30 min with the flow rate 10 mL/min. The peptide was detected by UV at λ = 215 nm. NMR spectra were recorded on a Bruker Avance 500 AV (Bruker Biospin, Switzerland) 500.1 MHz for ^1H and 125.8 MHz for ^{13}C. The chemical shifts are expressed in ppm relative to the shift of used solvent as an internal standard (^1H NMR, DMSO at 2.50 ppm, CH_3OH at 3.31 ppm and $CHCl_3$ at 7.26 ppm; ^{13}C NMR, $(CD_3)_2SO$ at 39.52 ppm, CD_3OD at 49.00 ppm and $CDCl_3$ at 77.16 ppm). Positive ion mass spectra were acquired with a quadrupole ion trap mass spectrometer (Finnigan MAT, San Jose, CA) equipped with an electrospray ionization source (ESI-MS). The purity of compound **14** was determined using Agilent 1100 HPLC (Agilent Technologies Inc., Waldbronn, Karlsruhe, Germany) with diode array detection, using reversed phase column (Zorbax Eclipse XDB C 18, 4.6 × 50 mm, 1.8 μm, Agilent Technologies, Palo Alto, CA, USA), 5% solvent B (0.05% AcOH in CH_3CN) in solvent A (0.05% AcOH in H_2O) for 5 min, then linear gradient 5−80% B in A in 15 min with the flow rate 1 mL/min. The purity of compound **15** was determined using Shimadzu LC-10Avp (Shimadzu, Kyoto, Japan), using a reverse phase column (Supelcogel ODP-50 C 18, 4 × 150 mm, 5 μm), with an isocratic eluent (0.05% AcOH, 2.5% MeOH, 97.45% H_20) in 30 min with the flow rate 1 mL/min. The purity of the rest of the compounds was determined by combustion analysis for CHN by Thermo Quest CE Instruments EA 1110 CHNS-O elemental analyzer. Peptide **14** showed 93% purity, and all other compounds had purity of ≥95%.

Manual Solid Phase Peptide Synthesis (SPPS). Wang resin (polymer-bound *p*-alkoxybenzyl alcohol) was used as solid support for the peptide synthesis of compounds **5** and **13**−**24**. Solid phase synthesis was performed in a 10 mL syringe equipped with a frit. Fmoc-Ala-Wang resin (loading 0.4−0.8 mmol/g) was swelled for 1 h in 3 mL of DMF. In the deprotection phase, the N^{α}-Fmoc protection group was removed with 5 mL of 20% (V/V) piperidine in DMF for 15 min and the resin was rinsed 5 times with DMF. In the coupling phase, the following N^{α}-Fmoc-amino acid or acetic acid (2−4 equiv) was preactivated (1−3 min) with the coupling reagent TBTU (2−4 equiv) and DIPEA (5−10 equiv) in 3−5 mL of DMF. This solution was added on the resin, and the syringe was shaken at rt for 60 min. Then the resin was rinsed 5 times with DMF. The cycle of Fmoc-deprotection and coupling was repeated until the desired resin-bound peptide was completed. Before cleavage from the resin, the resin was washed once with AcOH, five times with dichloromethane (DCM), and once with MeOH to remove the excess solvents and then dried under vacuum.

Cleavage of Peptide-Resin as Carboxylic Acid. The dried peptide-resin was preswelled in dioxane for 15 min. The excess of dioxane was removed, and 8 mL of cool (0 °C) cleavage mixture of 1 M NaOH (aq)/dioxane (2 and 6 mL) was added on the peptide-resin. The reaction mixture was shaken for 1 h at rt. The mixture was filtrated, the filtrate was collected and the resin was washed with H_2O/dioxane (1:3), dioxane and H_2O. The filtrate was neutralized with 3 M HCl (aq), and the solvents were evaporated. Acetone was added on the residue, and the mixture was filtrated to remove inorganic salts. The solvent of the filtrate was evaporated under reduced pressure to yield the crude product, which was purified by column chromatography or by crystallization.

Cleavage of Peptide-Resin as Methyl Ester. The dry peptide-resin was placed in a flask. Cleavage mixture DIPEA/MeOH/DMF (1:5:5, 11−22 mL) was added, and the reaction mixture was refluxed under argon atmosphere overnight. The mixture was filtrated, filtrate was collected and the resin was rinsed 5 times with MeOH/DMF (1:1). Solvent was evaporated from the combined filtrates under reduced pressure to yield the crude product, which was purified by column chromatography or by crystallization.

(*S*)-2-((*S*)-2-Acetamidopropanamido)-6-ethanethioamido-*N*-((*S*)-1-(methylamino)-1-oxopropan-2-yl)hexanamide (8). ^1H NMR ($(CD_3)_2SO$): δ = 1.15−1.21 (m, 6 H), 1.29 (m, 2 H), 1.45−1.73 (m, 4 H), 1.83 (s, 3 H), 2.37 (s, 3 H), 2.57 (d, 3 H), 3.43 (m, 2 H), 4.13−4.28 (m, 3 H), 7.73 (m, 1 H), 7.82 (d, 1 H), 7.92 (d, 1 H), 8.07 (d, 1 H), 9.93 (m, 1 H). ^{13}C NMR ($(CD_3)_2SO$): δ = 17.92, 18.29, 22.45, 22.81, 25.52, 26.81, 31.33, 32.77, 45.32, 48.08, 48.34, 52.36, 169.23, 170.98, 172.33, 172.55, 198.76. ESI-MS (m/z): 402.2 $[M + H]^+$, 424.3 $[M + Na]^+$. Anal. ($C_{17}H_{31}N_5O_4S \cdot 0.3$hexane$\cdot 0.2H_2O$) C, H, N.

(*S*)-Methyl 2-((*S*)-2-((*S*)-2-Acetamidopropanamido)-6-ethanethioamidohexanamido)propanoate (13). ^1H NMR (MeOD): δ = 1.34 (d, 3 H), 1.39 (d, 3 H), 1.47 (m, 2 H), 1.62−1.92 (m, 4 H), 1.98 (s, 3 H), 2.45 (s, 3 H), 3.59 (m, 2 H), 3.71 (s, 3 H), 4.28−4.45 (m, 3 H). ^{13}C NMR (MeOD): δ = 17.28, 17.80, 22.39, 24.06, 28.27, 32.86, 33.12, 46.96, 49.46, 50.63, 52.76, 54.12, 173.28, 173.92, 174.52, 175.18, 201.57. ESI-MS (m/z): 403.2 $[M + H]^+$, 425.3 $[M + Na]^+$. Anal. ($C_{17}H_{30}N_4O_5S$) C, H, N.

(*S*)-2-((*S*)-2-((*S*)-2-Aminopropanamido)-6-ethanethioamidohexanamido)propanoic Acid (14). ^1H NMR ($(CD_3)_2SO$): δ = 1.25 (d, 3 H), 1.28−1.41 (m, 2 H), 1.32 (d, 3 H), 1.48−1.74 (m, 4 H), 2.37 (s, 3 H), 3.42 (m, 2 H), 3.83 (m, 1 H), 4.09 (m, 1 H), 4.27 (m, 1 H), 8.12 (d, 1 H), 8.48 (d, 1 H), 9.99 (m, 1 H). ^{13}C NMR ($(CD_3)_2SO$): δ = 17.50, 17.55, 22.78, 26.95, 31.87, 32.81, 45.37, 47.95, 48.18, 52.51, 169.79, 170.62, 174.18, 198.83. ESI-MS (m/z): 347.14 $[M + H]^+$. HPLC: t_R 9.31 min, area percent 93% at 260 nm.

(*S*)-2-((*S*)-2-Amino-6-ethanethioamidohexanamido)propanoic Acid (15). ^1H NMR (D_2O): δ = 1.44 (d, 3 H), 1.50 (m, 2 H), 1.73 (m, 2 H), 1.96 (m, 2 H), 2.51 (s, 3 H), 3.63 (t, 2 H), 4.03 (t, 1 H), 4.36 (q, 1 H). ^{13}C NMR (D_2O): δ = 17.82, 22.71, 27.86, 31.87, 33.71, 47.11, 50.92, 54.36, 170.49, 178.16, 201.83. ESI-MS (m/z): 276.19 $[M + H]^+$. HPLC: t_R 3.18 min, area percent 99% at 260 nm.

(*S*)-Methyl 2-((*S*)-2-Acetamido-6-ethanethioamidohexanamido)propanoate (16). ^1H NMR ($CDCl_3$): δ = 1.43 (d, 3 H), 1.46 (m, 2 H), 1.66−1.88 (m, 4 H), 2.01 (s, 3 H), 2.56 (s, 3 H), 3.65 (m, 2 H), 3.76 (s, 3 H), 4.52 (m, 1 H), 4.57 (m, 1 H), 6.63 (m, 1 H), 7.12 (m, 1 H), 8.21 (m, 1 H). ^{13}C NMR ($CDCl_3$): δ = 17.47, 22.30, 23.13, 26.81, 32.62, 33.71, 45.84, 48.15, 52.30, 52.52, 170.45, 171.57, 173.31, 200.75. ESI-MS (m/z): 332.22 $[M + H]^+$, 354.25 $[M + Na]^+$. Anal. ($C_{14}H_{25}N_3O_4S \cdot 0.3Et_2O$) C, H, N.

(*S*)-2-((*S*)-2-((*S*)-1-Acetylpyrrolidine-2-carboxamido)-6-ethanethioamidohexanamido)propanoic Acid (17). ^1H NMR ($(CD_3)_2SO$): δ = 1.22−1.37 (m, 5 H), 1.46−1.79 (m, 5 H), 1.79−1.89 (m, 3 H), 1.96−2.22 (m, 3 H), 2.34−2.40 (m, 3 H), 3.37−3.59 (m, 4 H), 4.11−4.41 (m, 3 H), 7.85−7.94 (m, 1 H), 8.12−8.22 (m, 1 H), 9.86−9.97 (m, 1 H), 12.01−12.53 (br, 1 H). ^{13}C NMR ($(CD_3)_2SO$): δ = 16.97, 17.05, 21.03, 22.01, 22.38, 22.50, 22.76, 22.86, 24.31, 26.77, 26.79, 29.44, 31.28, 31.58, 31.73, 32.78, 45.27, 45.36, 46.29, 47.41, 47.47, 47.65, 51.71, 51.94, 59.34, 60.19, 168.51, 168.93, 171.27, 171.55, 171.80, 171.97, 173.91, 173.96, 198.77, 217.03. ESI-MS (m/z): 415.23 $[M + H]^+$. Anal. ($C_{18}H_{30}N_4O_5S \cdot 0.8$AcOH) C, H, N.

(6*S*,9*S*,12*S*)-9-(4-Ethanethioamidobutyl)-2,2,6,12-tetramethyl-4,7,10-trioxo-3-oxa-5,8,11-triazatridecan-13-oic Acid (18). ^1H NMR ($(CD_3)_2SO$): δ = 1.16 (d, 3 H), 1.26 (d, 3 H), 1.37 (s, 9 H), 1.22−1.41 (m, 2 H), 1.45−1.71 (m, 4 H), 2.37 (s, 3 H), 3.41 (m, 2 H), 3.96 (m, 1 H), 4.17 (m, 1 H), 4.28 (m, 1 H), 6.96 (d, 1 H), 7.69 (d, 1 H), 8.17 (d, 1 H), 9.90 (m, 1 H), 12.17 (br, 1 H). ^{13}C NMR ($(CD_3)_2SO$): δ = 17.09, 17.99, 21.04, 26.89, 28.17, 32.11, 32.79, 45.38, 47.45, 49.73, 51.75, 78.10, 155.07, 171.16, 171.98, 173.89, 198.75. ESI-MS (m/z): 447.11 $[M + H]^+$. Anal. ($C_{17}H_{30}N_4O_5S \cdot 0.6$AcOH$\cdot 0.1$5hexane) C, H, N.

(*S*)-2-((*S*)-2-((*R*)-2-Amino-3-phenylpropanamido)-6-ethanethioamidohexanamido)propanoic Acid (19). ^1H NMR ($(CD_3)_2SO$): δ = 1.15 (m, 2 H), 1.25 (d, 3 H), 1.38−1.61 (m, 4 H), 2.37 (s, 3 H), 2.66−3.00 (m, 2 H), 3.39 (m, 2 H), 3.68 (m, 1 H), 4.09 (m, 1 H), 4.25 (m, 1 H), 7.18−7.32 (m, 5 H), 8.19 (m, 2 H), 9.97 (m, 1 H). ^{13}C NMR ($(CD_3)_2SO$): δ = 17.43, 22.41, 26.86, 32.07, 32.76, 45.31, 47.82, 51.95, 55.15, 126.39, 128.18, 129.29, 137.49, 170.79, 171.88, 173.91, 198.74. ESI-MS (m/z): 423.27 $[M + H]^+$. Anal. ($C_{20}H_{30}N_4O_4S \cdot 0.5H_2O$) C, H, N.

(*S*)-2-((*S*)-2-(Benzyloxycarbonylamino)-6-ethanethioamidohexanamido)propanoic Acid (20). ^{1}H NMR ($(CD_3)_2SO$): δ = 1.27 (d, 3 H), 1.34 (m, 2 H), 1.45−1.69 (m, 4 H), 2.37 (s, 3 H), 3.43 (m, 2 H), 4.00 (m, 1 H), 4.19 (m, 1 H), 5.02 (s, 2 H), 7.27−7.42 (m, 6 H), 8.15 (d, 1 H), 9.92 (m, 1 H), 12.47 (br, 1 H). ^{13}C NMR ($(CD_3)_2SO$): δ = 17.11, 22.97, 26.89, 31.66, 32.79, 45.31, 47.38, 54.21, 65.31, 127.64, 127.74, 128.31, 137.05, 155.89, 171.67, 173.99, 198.74. ESI-MS (m/z): 410.26 $[M + H]^+$, 432.27 $[M + Na]^+$. Anal. ($C_{19}H_{27}N_3O_5S \cdot 0.1$hexane) C, H, N.

(*S*)-2-((*S*)-6-Ethanethioamido-2-(3-phenylpropanamido)hexanamido)propanoic Acid (21). ^{1}H NMR ($(CD_3)_2SO$): δ = 1.24 (m, 2 H), 1.27 (d, 3 H), 1.39−1.67 (m, 4 H), 2.37 (s, 3 H), 2.45 (m, 2 H), 2.80 (m, 2 H), 3.41 (m, 2 H), 4.18 (m, 1 H), 4.29 (m, 1 H), 7.13−7.29 (m, 5 H), 7.93 (d, 1 H), 8.17 (d, 1 H), 9.90 (m, 1 H), 12.47 (br, 1 H). ^{13}C NMR ($(CD_3)_2SO$): δ = 17.03, 22.73, 26.92, 31.07, 31.93, 32.78, 36.68, 45.37, 47.35, 51.84, 125.81, 128.18, 128.19, 141.27, 171.21, 171.49, 173.96, 198.72. ESI-MS (m/z): 408.23 $[M + H]^+$. Anal. ($C_{20}H_{29}N_3O_4S \cdot 0.1H_2O \cdot 0.1$hexane) C, H, N.

(*S*)-2-((*S*)-6-Ethanethioamido-2-(3-(2-fluorophenyl)propanamido)hexanamido)propanoic Acid (22). ^{1}H NMR ($(CD_3)_2SO$): δ = 1.19−1.31 (m, 2 H), 1.26 (d, 3 H), 1.41−1.67 (m, 4 H), 2.37 (s, 3 H), 2.44 (m, 2 H), 2.82 (dd, 2 H), 3.40 (m, 2 H), 4.18 (m, 1 H), 4.28 (m, 1 H), 7.06−7.16 (m, 2 H), 7.19−7.32 (m, 2 H), 7.97 (d, 1 H), 8.18 (d, 1 H), 9.90 (m, 1 H), 12.33 (br, 1 H). ^{13}C NMR ($(CD_3)_2SO$): δ = 17.03, 22.74, 24.17 (J_{CF} = 2.49 Hz), 26.91, 31.90, 32.78, 35.06, 45.36, 47.36, 51.89, 114.98 (d, J_{CF} = 21.88 Hz), 124.24 (d, J_{CF} = 3.32 Hz), 127.77 (d, J_{CF} = 15.72 Hz), 127.96 (d, J_{CF} = 8.09 Hz), 130.58 (J_{CF} = 4.89 Hz), 160.43 (J_{CF} = 243.12 Hz), 170.87, 171.47, 173.98, 198.73. ESI-MS (m/z): 426.23 $[M + H]^+$. Anal. ($C_{20}H_{28}FN_3O_4S \cdot 0.4$AcOH $\cdot 0.05$hexane) C, H, N.

(*S*)-2-((*S*)-6-Ethanethioamido-2-(3-(2-hydroxyphenyl)propanamido)hexanamido)propanoic Acid (23). ^{1}H NMR ($(CD_3)_2SO$): δ = 1.21−1.33 (m, 2 H), 1.27 (d, 3 H), 1.42−1.68 (m, 4 H), 2.37 (s, 3 H), 2.39 (m, 2 H), 2.72 (dd, 2 H), 3.41 (m, 2 H), 4.18 (m, 1 H), 4.29 (m, 1 H), 6.68 (m, 1 H), 6.76 (d, 1 H), 6.98 (m, 1 H), 7.04 (d, 1 H), 7.91 (d, 1 H), 8.17 (d, 1 H), 9.28 (br, 1 H), 9.91 (m, 1 H), 12.29 (br, 1 H). ^{13}C NMR ($(CD_3)_2SO$): δ = 17.05, 22.79, 25.62, 26.92, 31.89, 32.79, 35.09, 45.36, 47.39, 51.91, 114.87, 118.83, 126.88, 127.41, 129.54, 155.02, 171.54, 171.75, 173.98, 198.73. ESI-MS (m/z): 424.20 $[M + H]^+$. Anal. ($C_{20}H_{29}N_3O_5S \cdot 0.1H_2O \cdot 0.7$AcOH) C, H, N.

(*S*)-2-((*S*)-2-((*R*)-1-(*tert*-Butoxycarbonyl)piperidine-3-carboxamido)-6-ethanethioamidohexanamido)propanoic Acid (24). ^{1}H NMR ($(CD_3)_2SO$): δ = 1.26 (d, 3 H), 1.21−1.37 (m, 4 H), 1.39 (s, 9 H), 1.43−1.86 (m, 6 H), 2,32 (m, 1 H), 2.37 (s, 3 H), 2.59−2.85 (m, 2 H), 3.43 (m, 2 H), 3.78−3.97 (m, 2 H), 4.16 (m, 1 H), 4.24 (m, 1 H), 7.98 (d, 1 H), 8.09 (m, 1 H), 9.92 (m, 1 H), 12.36 (br, 1 H). ^{13}C NMR ($(CD_3)_2SO$): δ = 17.11, 21.03, 22.79, 22.84, 24.10 (br), 26.88, 27.44, 28.04, 31.73, 32.78, 41.86, 45.33, 47.38, 51.79, 78.65, 153.80, 171.39, 172.68, 173.99, 198.75. ESI-MS (m/z): 487.12 $[M + H]^+$, 509.32 $[M + Na]^+$. Anal. ($C_{22}H_{38}N_4O_6S \cdot 0.4$AcOH $\cdot 0.2$hexane) C, H, N.

(*S*)-Benzyl 1-(Cyclohexylamino)-6-ethanethioamido-1-oxohexan-2-ylcarbamate (27). ^{1}H NMR ($CDCl_3$): δ = 1.04−1.95 (m, 16 H), 2.54 (s, 3 H), 3.55−3.78 (m, 3 H), 4.09 (m, 1 H), 5.11 (s, 2 H), 5.45 (d, 1 H), 5.86 (d, 1 H), 7.29−7.39 (m, 5 H), 7.72 (m, 1 H). ^{13}C NMR ($CDCl_3$): δ = 22.67, 24.88, 25.54, 26.99, 32.56, 33.01, 33.12, 34.22, 45.89, 48.64, 54.51, 67.28, 128.15, 128.45, 128.74, 136.23, 156.59, 170.52, 201.08. ESI-MS (m/z): 420.30 $[M + H]^+$, 442.32 $[M + Na]^+$. Anal. ($C_{22}H_{33}N_3O_3S$) C, H, N.

(*S*)-Benzyl 6-Ethanethioamido-1-(2-fluorophenylamino)-1-oxohexan-2-ylcarbamate (28). ^{1}H NMR ($CDCl_3$): δ = 1.50 (m, 2 H), 1.66−2.05 (m, 4 H), 2.53 (s, 3 H), 3.66 (m, 2 H), 4.36 (m, 1 H), 5.15 (s, 2 H), 5.43 (d, 1 H), 7.03−7.16 (m, 3 H), 7.28−7.40 (m, 5 H), 7.53 (br, 1 H), 8.11 (br, 1 H), 8.19 (dd, 1 H). ^{13}C NMR ($CDCl_3$): δ = 22.82, 27.23, 31.89, 34.30, 45.81, 55.42, 67.65, 115.18 (d, J = 19.17 Hz), 122.21, 124.70 (d, J = 3.65 Hz), 125.25 (d, J = 7.63 Hz), 125.77 (J = 10.05 Hz), 128.25, 128.54, 128.77, 135.98, 152.94 (J = 244.37), 156.77, 170.04, 201.24. ESI-MS (m/z): 432.26 $[M + H]^+$. Anal. ($C_{22}H_{26}FN_3O_3S \cdot 0.2H_2O$) C, H, N.

(*S*)-Benzyl 6-Ethanethioamido-1-(2-hydroxyphenylamino)-1-oxohexan-2-ylcarbamate (29). ^{1}H NMR ($CDCl_3$): δ = 1.47 (m, 2 H), 1.64−2.02 (m, 4 H), 2.51 (s, 3 H), 3.66 (s, 2 H), 4.41 (br, 1 H), 5.13 (s, 2 H), 5.52 (d, 1 H), 6.86 (dd, 1 H), 6.98 (d, 1 H), 7.11 (dd, 2 H), 7.28−7.40 (m, 5 H), 7.52 (br, 1 H), 8.33 (s, 1 H), 8.55 (br, 1 H). ^{13}C NMR ($CDCl_3$): δ = 22.71, 27.23, 31.84, 34.31, 45.67, 55.12, 67.78, 119.45, 120.85, 122.74, 125.19, 127.47, 128.28, 128.61, 128.81, 135.88, 148.52, 156.83, 171.58, 201.38. ESI-MS (m/z): 430.23 $[M + H]^+$. Anal. ($C_{22}H_{27}N_3O_4S$) C, H, N.

(*S*)-Benzyl 6-Ethanethioamido-1-oxo-1-(2-oxo-2-phenylethylamino)hexan-2-ylcarbamate (30). ^{1}H NMR ($CDCl_3$): δ = 1.50 (m, 2 H), 1.65−1.98 (m, 4 H), 2.53 (s, 3 H), 3.64 (m, 2 H), 4.35 (m, 1 H), 4.76 (m, 2 H), 5.14 (s, 2 H), 5.54 (d, 1 H), 6.95 (br, 1 H), 7.28−7.39 (m, 5 H), 7.51 (dd, 2 H), 7.64 (dd, 1 H), 7.74 (br, 1 H), 7.96 (d, 2 H). ^{13}C NMR ($CDCl_3$): δ = 22.72, 27.11, 32.83, 34.21, 46.07, 46.45, 54.49, 67.37, 128.09, 128.18, 128.45, 128.75, 129.16, 134.39, 134.48, 136.18, 156.55, 171.86, 194.05, 201.13. ESI-MS (m/z): 456.26 $[M + H]^+$. Anal. ($C_{24}H_{29}N_3O_4S$) C, H, N.

In Vitro Assay for SIRT1 and SIRT2 Activities. The Fluor de Lys fluorescence assays were based on the method described in the BioMol product sheet using BioMol KI177 substrate for SIRT1 and KI179 substrate for SIRT2. Determined K_m for SIRT1 substrate was 58 μM and for SIRT2 substrate 198 μM.[16]

Briefly, assays were carried out using Fluor de Lys acetylated 40 μM SIRT1- or 138 μM SIRT2-peptide substrate (concentrations were 70% of K_m values), 500 μM NAD^+ (N6522, Sigma), recombinant GST-SIRT1/2-enzyme and SIRT assay buffer (HDAC assay buffer, KI143, supplemented with 1 mg/mL bovine serum albumin (BSA), A3803, Sigma). GST-SIRT1-enzyme and GST-SIRT2-enzyme were produced as described recently.[39,40] The buffer, SIRT1/2-peptide substrate, NAD^+ and dimethyl sulfoxide (DMSO)/compounds in DMSO (2.5 μL in 50 μL total volume of reaction mixture; DMSO from Sigma, D2650) for testing were preincubated for 5 min at rt. The reaction was started by adding the SIRT1- or SIRT2-enzyme. The reaction mixture was incubated for 1 h at 37 °C. After that Fluor de Lys developer (KI176) plus 2 mM nicotinamide in 50 μL were added and incubation was continued for 45 min at 37 °C. Fluorescence readings were obtained using the Victor 1420 Multilabel Counter (Wallac, Finland) with excitation wavelength 355 nm and emission 460 nm.

The IC_{50} values were based on 9-point dose−response determination (2000 μM, 1000 μM, 100 μM, 10 μM, 1 μM, 0.1 μM, 0.01 μM, 0.001 μM and 0.0001 μM) where more necessary dose points were added between the critical concentrations depending on the compound. Each experiment was repeated at least three times and calculated using Graph Pad Prism Software version 4.03 (19922005 GraphPad Software, Inc.). The SIRT1 and SIRT2 assays differ in their active enzyme concentrations, and consequently, SIRT1 and SIRT2 IC_{50} values cannot be directly compared.

In Vitro Assay for HDAC Activities. The Fluor de Lys fluorescence assay was based on the method described in the product sheet for HDAC Fluorimetric Assay/Drug Discovery Kit of Enzo Life Sciences (BML-AK500).

Briefly, assay was carried out using Fluor de Lys acetylated 50 μM HDAC-peptide substrate, human cervical cancer cell line (HeLa) nuclear extract dilution as recommended in the kit and 200 μM test compounds diluted in HDAC assay buffer. The reaction was started by adding the substrate as recommended in the kit protocol. The reaction mixture was incubated for 1 h at 37 °C. After that Fluor de Lys developer plus 1 μM nicotinamide was added and incubation was continued for 15 min at 25 °C. Fluorescence readings were obtained using the Victor 1420 Multilabel Counter (Wallac, Finland) with excitation wavelength 355 nm and emission 460 nm.

The experiment was repeated twice. Means and standard deviations were calculated using SPSS Software version 14.0 for Windows (IBM Corporation, USA).

Cell Culture. Clonetics normal human astrocytes (NHA) were purchased from Lonza (Basel, Switzerland). Cells were cultured in Dulbecco's modified Eagle medium (DMEM) (Sigma, St. Louis, MO, USA) with the astrocyte growth medium (AGM) supplement (Lonza, Basel, Switzerland), 10% fetal bovine serum (Lonza), 100 units/mL penicillin (Lonza), 100 μg/mL streptomycin (Lonza), and 2 mM glutamine (Lonza). Human retinal pigment epithelial cells (ARPE-19) were obtained from American Type Culture Collection (ATCC). The cells were grown in DMEM/Nut MIX F-12 medium (Lonza) including 10% fetal bovine serum (Hyclone, Logan, UT, USA), 100 units/mL penicillin, 100 μg/mL streptomycin, and 2 mM glutamine. SH-SY5Y neuroblastomas (DSMZ, Braunschweig, Germany) were cultured in 50% DMEM−50% optimized modified Eagle medium (OPTI-MEM) (Gibco, Rockville, MD, USA) containing 5% fetal bovine serum, 100 units/mL penicillin (Lonza), 100 μg/mL streptomycin (Lonza), and 2 mM glutamine (Lonza). All cell types were plated to 12-well plates (Nunc, Roskilde, Denmark) at density 10^5 cells/well, and the experiments were initiated after 24 h. Test compounds and etoposide (Sigma, St. Louis, MO, USA) were added at the same time and incubated for 5 h before harvesting.

Western Blotting. For the Western blot analysis, the cells were lysed into the M-PER Mammalian Protein Extraction Reagent (Thermo Fisher Scientific, Waltham, MA, USA). Before estimation of protein levels with the DC protein assay kit (Bio-Rad Laboratories, Hercules, CA, USA) the lysates were centrifuged at 16000*g* for 20 min. Equal amounts of total protein were electrophoretically separated in 4−12% SDS−PAGE gel (Invitrogen, Carlsbad, CA, USA). Subsequently, proteins were transferred onto Hybond-ECL nitrocellulose transfer membrane (Amersham, GE Healthcare, London, U.K.) using electroblotting (Trans-Blot Cell wet blotting apparatus, Bio-Rad Laboratories, Hercules, CA, USA). The specific protein was detected with rabbit monoclonal acetyl-p53 (K382) antibody (Abcam, Cambridge, U.K.). Actin (H-196, sc-7210, Santa Cruz, CA, USA) was used as loading control. The staining of specific proteins was carried out using horseradish peroxidase (HRP)-linked secondary antibody (donkey-anti-rabbit, NA934, GE Healthcare, London, U.K.) and chemiluminescent substrate (Immobilon Western Chemiluminescent HRP Substrate, Millipore, Billerica, MA, USA). Filters were exposed to a medical X-ray film (SuperRX-film, Fujifilm Corporation, Tokyo, Japan), developed with Kodak X-OMAT 2000 developing machine (Eastman Kodak Company, Rochester, NY, USA) and scanned with the Epson Perfection V750 Pro scanner (Epson America Inc., Long Beach, CA, USA) using Jasc Paint Shop Pro 8 software (Jasc Software Inc., Eden Prairie, MN, USA). Images were processed with the use of UN-SCAN-IT gel software (Silk Scientific Corporation, Orem, UT, USA).

Lactate Dehydrogenase Assay. Lactate dehydrogenase (LDH) leakage from the cells to medium was used as a marker for cytotoxicity. LDH was measured from cell culture medium with the cytotoxicity kit obtained from Promega (G1780).

■ ASSOCIATED CONTENT

Supporting Information. Detailed experimental procedures for the syntheses and NMR spectra for the compounds **4**−**24** and **26**−**30**, ESI-MS results, elemental analysis data and additional docking pose figures. This material is available free of charge via the Internet at http://pubs.acs.org.

■ AUTHOR INFORMATION

Corresponding Author

*Tel: +358 40 3553693. Fax: +358 17 162424. E-mail: Heikki.Salo@uef.fi.

Author Contributions

‡These authors contributed equally to this work.

■ ACKNOWLEDGMENT

We thank Prof. Kristina Luthman for helpful discussions during this work and M.Sc. Marko Lehtonen, Tanja Bruijn, Miia Reponen, Tiina Koivunen and Anneleena Holopainen for their skillfull assistance. We thank the Graduate School of Drug Discovery, Academy of Finland (Grants 127062 and 132780), Orion Farmos Research Foundation, Finnish Cultural Foundation, Emil Aaltonen Foundation and the Saastamoinen Foundation for financial support. We thank Biocenter Kuopio for the facilities and the CSC-IT center of Science Limited for providing software licenses for the Shcrödinger software package. This work is part of COST Action TD09056: "Epigenetics: Bench to Bedside".

■ ABBREVIATIONS USED

SIRT1−7, human silent information regulator type 1−7; Sir2Tm, silent information regulator 2 *Thermotoga maritima*; NAD+, nicotinamide adenine dinucleotide; cbz, carbonyloxybenzyl; fmoc, 9-fluorenylmethoxycarbonyl; SPPS, solid phase peptide synthesis; DIPEA, *N*,*N*-diisopropylethylamine; DMF, *N*,*N*-dimethylformamide; TBTU, *O*-(benzotriazol-1-yl)-*N*,*N*,*N*′,*N*′-tetramethyluronium tetrafluoroborate; SAR, structure activity relationship; rmsd, root-mean-square deviation; Boc, *tert*-butoxycarbonyl; HDAC, histone deacetylase; SH-SY5Y, human derived neuroblastoma cell line; DMSO, dimethyl sulfoxide; DCM, dichloromethane; GST, glutathione-*S*-transferase; BSA, bovine serum albumin; DMEM, Dulbecco's modified Eagle medium; AGM, astrocyte growth medium; OPTI-MEM, optimized modified Eagle medium; SDS−PAGE, sodium dodecyl sulfate polyacrylamide gel electrophoresis; HRP, horseradish peroxidase; LDH, lactate dehydrogenase

■ REFERENCES

(1) Haigis, M. C.; Sinclair, D. A. Mammalian sirtuins: biological insights and disease relevance. *Annu. Rev. Pathol.* **2010**, *5*, 253–295.

(2) Lavu, S.; Boss, O.; Elliott, P. J.; Lambert, P. D. Sirtuins—novel therapeutic targets to treat age-associated diseases. *Nat. Rev. Drug Discovery* **2008**, *7*, 841–853.

(3) Milne, J. C.; Lambert, P. D.; Schenk, S.; Carney, D. P.; Smith, J. J.; Gagne, D. J.; Jin, L.; Boss, O.; Perni, R. B.; Vu, C. B.; Bemis, J. E.; Xie, R.; Disch, J. S.; Ng, P. Y.; Nunes, J. J.; Lynch, A. V.; Yang, H.; Galonek, H.; Israelian, K.; Choy, W.; Iffland, A.; Lavu, S.; Medvedik, O.; Sinclair, D. A.; Olefsky, J. M.; Jirousek, M. R.; Elliott, P. J.; Westphal, C. H. Small molecule activators of SIRT1 as therapeutics for the treatment of type 2 diabetes. *Nature* **2007**, *450*, 712–716.

(4) Taylor, D. M.; Maxwell, M. M.; Luthi-Carter, R.; Kazantsev, A. G. Biological and potential therapeutic roles of sirtuin deacetylases. *Cell. Mol. Life Sci.* **2008**, *65*, 4000–4018.

(5) Peck, B.; Chen, C. Y.; Ho, K. K.; Di Fruscia, P.; Myatt, S. S.; Coombes, R. C.; Fuchter, M. J.; Hsiao, C. D.; Lam, E. W. SIRT inhibitors induce cell death and p53 acetylation through targeting both SIRT1 and SIRT2. *Mol. Cancer Ther.* **2010**, *9*, 844–855.

(6) Neugebauer, R. C.; Sippl, W.; Jung, M. Inhibitors of NAD+ dependent histone deacetylases (sirtuins). *Curr. Pharm. Des.* **2008**, *14*, 562–573.

(7) Mai, A.; Altucci, L. Epi-drugs to fight cancer: from chemistry to cancer treatment, the road ahead. *Int. J. Biochem. Cell Biol.* **2009**, *41*, 199–213.

(8) Guarani, V.; Potente, M. SIRT1—a metabolic sensor that controls blood vessel growth. *Curr. Opin. Pharmacol.* **2010**, *10*, 139–145.

(9) Alcain, F. J.; Villalba, J. M. Sirtuin inhibitors. *Expert Opin. Ther. Pat.* **2009**, *19*, 283–294.

(10) Luthi-Carter, R.; Taylor, D. M.; Pallos, J.; Lambert, E.; Amore, A.; Parker, A.; Moffitt, H.; Smith, D. L.; Runne, H.; Gokce, O.; Kuhn, A.;

Xiang, Z.; Maxwell, M. M.; Reeves, S. A.; Bates, G. P.; Neri, C.; Thompson, L. M.; Marsh, J. L.; Kazantsev, A. G. SIRT2 inhibition achieves neuroprotection by decreasing sterol biosynthesis. *Proc. Natl. Acad. Sci. U.S.A.* **2010**, *107*, 7927–7932.

(11) Outeiro, T. F.; Kontopoulos, E.; Altmann, S. M.; Kufareva, I.; Strathearn, K. E.; Amore, A. M.; Volk, C. B.; Maxwell, M. M.; Rochet, J. C.; McLean, P. J.; Young, A. B.; Abagyan, R.; Feany, M. B.; Hyman, B. T.; Kazantsev, A. G. Sirtuin 2 inhibitors rescue alpha-synuclein-mediated toxicity in models of Parkinson's disease. *Science* **2007**, *317*, 516–519.

(12) Fatkins, D. G.; Monnot, A. D.; Zheng, W. Nepsilon-thioacetyl-lysine: a multi-facet functional probe for enzymatic protein lysine Nepsilon-deacetylation. *Bioorg. Med. Chem. Lett.* **2006**, *16*, 3651–3656.

(13) Fatkins, D. G.; Zheng, W. Substituting N-thioacetyl-lysine for N-acetyl-lysine in peptide substrates as a general approach to inhibiting human NAD-dependent protein deacetylases. *Int. J. Mol. Sci.* **2008**, *9*, 1–11.

(14) Smith, B. C.; Denu, J. M. Acetyl-lysine analog peptides as mechanistic probes of protein deacetylases. *J. Biol. Chem.* **2007**, *282*, 37256–37265.

(15) Suzuki, T.; Asaba, T.; Imai, E.; Tsumoto, H.; Nakagawa, H.; Miyata, N. Identification of a cell-active non-peptide sirtuin inhibitor containing N-thioacetyl lysine. *Bioorg. Med. Chem. Lett.* **2009**, *19*, 5670–5672.

(16) Kiviranta, P. H.; Suuronen, T.; Wallén, E. A. A.; Leppänen, J.; Tervonen, J.; Kyrylenko, S.; Salminen, A.; Poso, A.; Jarho, E. M. N(epsilon)-thioacetyl-lysine-containing tri-, tetra-, and pentapeptides as SIRT1 and SIRT2 inhibitors. *J. Med. Chem.* **2009**, *52*, 2153–2156.

(17) Huhtiniemi, T.; Suuronen, T.; Lahtela-Kakkonen, M.; Bruijn, T.; Jääskeläinen, S.; Poso, A.; Salminen, A.; Leppänen, J.; Jarho, E. N(epsilon)-Modified lysine containing inhibitors for SIRT1 and SIRT2. *Bioorg. Med. Chem.* **2010**, *18*, 5616–5625.

(18) Smith, B. C.; Denu, J. M. Mechanism-based inhibition of Sir2 deacetylases by thioacetyl-lysine peptide. *Biochemistry* **2007**, *46*, 14478–14486.

(19) Smith, B. C.; Denu, J. M. Sir2 deacetylases exhibit nucleophilic participation of acetyl-lysine in NAD+ cleavage. *J. Am. Chem. Soc.* **2007**, *129*, 5802–5803.

(20) McGregor, D. P. Discovering and improving novel peptide therapeutics. *Curr. Opin. Pharmacol.* **2008**, *8*, 616–619.

(21) Asaba, T.; Suzuki, T.; Ueda, R.; Tsumoto, H.; Nakagawa, H.; Miyata, N. Inhibition of human sirtuins by in situ generation of an acetylated lysine-ADP-ribose conjugate. *J. Am. Chem. Soc.* **2009**, *131*, 6989–6996.

(22) Huhtiniemi, T.; Wittekindt, C.; Laitinen, T.; Leppänen, J.; Salminen, A.; Poso, A.; Lahtela-Kakkonen, M. Comparative and pharmacophore model for deacetylase SIRT1. *J. Comput.-Aided. Mol. Des.* **2006**, *20*, 589–599.

(23) Finnin, M. S.; Donigian, J. R.; Pavletich, N. P. Structure of the histone deacetylase SIRT2. *Nat. Struct. Biol.* **2001**, *8*, 621–625.

(24) Jin, L.; Wei, W.; Jiang, Y.; Peng, H.; Cai, J.; Mao, C.; Dai, H.; Choy, W.; Bemis, J. E.; Jirousek, M. R.; Milne, J. C.; Westphal, C. H.; Perni, R. B. Crystal structures of human SIRT3 displaying substrate-induced conformational changes. *J. Biol. Chem.* **2009**, *284*, 24394–24405.

(25) Cosgrove, M. S.; Bever, K.; Avalos, J. L.; Muhammad, S.; Zhang, X.; Wolberger, C. The structural basis of sirtuin substrate affinity. *Biochemistry* **2006**, *45*, 7511–7521.

(26) *MOE (The Molecular Operating Environment)*, Version 2008.10 and 2009.10; software available from Chemical Computing Group Inc., 1010 Sherbrooke Street West, Suite 910, Montreal, Canada H3A 2R7. http://www.chemcomp.com.

(27) Solomon, J. M.; Pasupuleti, R.; Xu, L.; McDonagh, T.; Curtis, R.; DiStefano, P. S.; Huber, L. J. Inhibition of SIRT1 catalytic activity increases p53 acetylation but does not alter cell survival following DNA damage. *Mol. Cell. Biol.* **2006**, *26*, 28–38.

(28) *LigPrep*, version 2.3; Schrödinger, LLC: New York, NY, 2009.

(29) *Epik*, version 2.0; Schrödinger, LLC: New York, NY, 2009.

(30) *CombiGlide*, version 2.5; Schrödinger, LLC: New York, NY, 2009.

(31) *Glide*, version 5.5; Schrödinger, LLC: New York, NY, 2009.

(32) *Schrödinger Suite 2009 Protein Preparation Wizard, Epik version 2.0; Impact version 5.5; Prime version 2.1*; Schrödinger, LLC: New York, NY, 2009.

(33) Kerwin, S. M. ChemBioOffice Ultra 2010 suite. *J. Am. Chem. Soc.* **2010**, *132*, 2466–2467.

(34) *Discovery Studio Modeling Environment*, Release 2.5; Accelrys Software Inc.: San Diego, 2009.

(35) The Universal Protein Resource (UniProt) in 2010. *Nucleic Acids Res.* **2010**, *38*, D142−148.

(36) Larkin, M. A.; Blackshields, G.; Brown, N. P.; Chenna, R.; McGettigan, P. A.; McWilliam, H.; Valentin, F.; Wallace, I. M.; Wilm, A.; Lopez, R.; Thompson, J. D.; Gibson, T. J.; Higgins, D. G. Clustal W and Clustal X. *Bioinformatics* **2007**, *23*, 2947–2948.

(37) Waterhouse, A. M.; Procter, J. B.; Martin, D. M.; Clamp, M.; Barton, G. J. Jalview Version 2—a multiple sequence alignment editor and analysis workbench. *Bioinformatics* **2009**, *25*, 1189–1191.

(38) *rmsd.py version 1.14.2.6, Maestro version 9.1*; Schrodinger, LLC: New York, NY, 2010.

(39) Tervo, A. J.; Kyrylenko, S.; Niskanen, P.; Salminen, A.; Leppänen, J.; Nyrönen, T. H.; Järvinen, T.; Poso, A. An in silico approach to discovering novel inhibitors of human sirtuin type 2. *J. Med. Chem.* **2004**, *47*, 6292–6298.

(40) Kiviranta, P. H.; Leppänen, J.; Rinne, V. M.; Suuronen, T.; Kyrylenko, O.; Kyrylenko, S.; Kuusisto, E.; Tervo, A. J.; Järvinen, T.; Salminen, A.; Poso, A.; Wallén, E. A. A. N-(3-(4-Hydroxyphenyl)-propenoyl)-amino acid tryptamides as SIRT2 inhibitors. *Bioorg. Med. Chem. Lett.* **2007**, *17*, 2448–2451.